AASE PROCEEDING

2020 AASE INTERNATIONAL CONFERENCE

International Conference on Engineering, Technology and Applied Science (ETAS)

International Conference on Business, Education, Social Science, and Management (BESM)

| ETAS-55/BESM-56 | MAY 19-20 | 2020 | TAIPEI/TAIWAN |

PROCEEDINGS OF
AASE INTERNATIONAL
CONFERENCE
55th ETAS & 56th BESM Conference

Applied and Advanced Science Exchange
(AASE)

International Conference on Engineering, Technology and Applied Science (ETAS)

- 55th ETAS @ Taipei/Taiwan, May.19th-20th, 2020

International Conference on Business, Education, Social Science, and Management (BESM)

- 56th BESM @ Taipei/Taiwan, May.19th-20th, 2020

Applied and Advanced Science Exchange (AASE):

The *Applied and Advanced Science Exchange* (AASE) is an active professional community and registered as a non-profit organization (NGO) in Japan. AASE has devoted itself to disseminate a variety of knowledge and worked with a vision to share the innovations in fields of academia by building up an international platform. Nowadays, interdisciplinary research is increasing and playing a key role. In our interdisciplinary joint conferences, participants are able to share their viewpoints from different perspectives and seek new collaborative opportunities across fields.

The *Applied and Advanced Science Exchange* (AASE) offers an extraordinary platform for networking opportunities and discussions to enhance research progress in various fields. From 2016, we have run a series of professional workshops, conferences, seminars and symposiums, and have built a reputation for delivering inspirational conferences with flawless execution. Our purpose is to facilitate networking opportunities for scholars and be the information resources for dynamic professional development opportunities throughout the World.

AASE conferences footprints of the world

EDITORIAL MESSAGE

It is my proud privilege to welcome you all to the AASE International Conference at Taipei/Taiwan on 19th-20th May, 2020. AASE International Conference serves as platform that aims to provide opportunity to the academicians and scholars from across various disciplines to discuss interdisciplinary innovations. We are happy to see the papers from all part of the world published in this proceedings. This proceeding brings out the various Research papers from diverse areas of science, engineering, technology, management, business and education. These articles that we received for these conferences are very promising and impactful. We believe these studies have the potential to address key challenges in various sub-domains of social sciences and applied sciences. I am really thankful to all the participants for being here with us to create an environment of knowledge sharing and learning. I am also thankful to our scientific and review committee for spending much of their time in reviewing the papers for these events. I am sure the contributions by the authors shall add value to the research community.

Editor-In-Chief
Dr. H. Miyamoto

TABLE OF CONTENTS

★★★

Flood Mitigation and Program Implementation in the Municipality of Calasiao Pangasinan Philippines

Gudelia M. Samson, Dpa

Pangasinan State University

Abstract

The study aimed to determine the extent of implementation of the flood mitigation and control program in the Municipality of Calasiao Pangasinan, Philippines along mitigation and preparedness, response and rehabilitation. This is a descriptive research which used a survey questionnaire designed according to the problem set in the study. The questionnaire consisted of two (2) parts. The first part dwelt on the extent of implementation of flood mitigation and control program in the Municipality of Calasiao, along with its three phases. The second part dwelt on the weaknesses cited in the implementation of flood mitigation and control program, along with its three phases. An interview was done in the informal manner. Perceptions were obtained from 65 respondents for the calendar years 2012-2015. The respondents of the study includes all the implementers or members of the Municipal Disaster Risk Reduction Management Council of Calasiao Pangasinan, Philippines which composed of 21 members in accordance with RA 10121 while the total number of Barangay DRRMC and 2 civil society organizations representatives. The population of 6 barangays numbered to a total of 66. The data were treated and analyzed through the use of average weighted mean, percentage technique and ranking to determine the extent of implementation of the flood mitigation and control program as well as the weakness cited in the implementation of the program in the Municipality of Calasiao Pngasinan, Philippines. The results from the study served as basis for designing a manageable and viable municipal risk reduction and management program toward flood free municipality of Calasiao Pangasinan, Philippines.

The Impact of Taiwan Stock Market on Bitcoin Price under the NonLinear of Taiwan's Monetary Policy

Tzu-Yi Yang[a]

[a]Department of Business and Management, Ming Chi University of Technology, Taiwan

Email: tyyang@mail.mcut.edu.tw

Abstract

This study proposes a smooth transition autoregressive model (STARX) with exogenous variables to study the non-linear relationship between Taiwan's monetary policy threshold and the Taiwan stock market from February 2, 2012 to August 31, 2019 . Threshold effects indicate that the relationship between oil prices and their production is non-linear, and changes over time and between Bitcoin and Taiwan's stock markets and transition variables are different. In addition, thresholds do exist. In addition, according to the threshold, Bitcoin's response to the Taiwan stock market is asymmetric. In the end, when there is a two-cycle lag in the closing price of Taiwan Exchange under the influence of the threshold effect of Taiwan 's monetary policy, it has a non-linear effect on the closing price of Bitcoin. In contrast, when TAIEX closing price returns have a three-cycle lag, there is no threshold for the effect of TAIEX closing prices returns on TAIEX closing prices returns.

Keywords: Nonlinear, Bitcoin, Stock market, Monetary policy

3D vision combined with Internet of Things in geometric feature measurement system

Wei-Wen Chen , Ko-Shyang Wang , Chien-Chun Kuo , Tsai-Ling Kao , Chung-Li Tai , Chih-Kai Chiu , and Kai-Siang Gan[a]

Research Institute Southern Region Campus, Smart Microsystems Tech-nology Center,

Visual Interaction Dept., Taiwan

[a]Corresponding author: PeterGan@itri.org.tw

Abstract

Based on the Internet of Things, this study developed a feeding management system and applied it to monitoring the growth of calves. The sensor module includes a 3D visual sensor module, gas sensor, and load cell sensor module. All data and images received are transmitted to the data collection server computer via cables, interfaced with the Calf Guide feeding data, then simultaneously uploaded to the feeding management system. The feeding management system developed not only displays data on calf growth such as length, width, height, weight, and milk intake, but also uses cloud computing and data analysis combined with feeding experience to provide daily personified judgment and suggestions when calves enter the milk-drinking sensor area as an important reference for improving feeding efficiency.

Keywords: Internet of Things, 3D Visual module, load cells, Feeding and Management

---

1. Introduction

Dairy farming is a live animal raising business that operates 7 days a week all year round. The feeding, management, behavior monitoring and identification processes each rely on a great deal of manpower and time. As economy and society advance, this industry's long work hours, high manual labor requirement, and poor work environments have resulted in labor shortage problems. The Council of Agriculture's proposal to readmit foreign laborers to the dairy farming industry attracted large attention, and farms in Taiwan have also gradually introduced automated equipment from overseas, such as milking machines, feeders, and manure scrapers, to reduce the risks caused by labor shortage. In the future, the industry structure will grow from labor intensive towards technology and capital intensive professional op-eration. By introducing automated equipment, manpower can be cut back, solving the dairy farmers' extended problem of labor shortage. Means for leveraging existing resources to add value to these automated equipment and to develop a system for local raising environments through technology such as Internet mechanisms, cloud computing, and data analysis not only increase the economic value of the equipment, but also reduce the cost of automation in the long run. They are becoming the key to dairy farm intellectualizing upgrades as well.

In this study, a feeding management system is developed which combines a 3D visual module, load cell sensor module, gas sensor, and automated feeder. The main application is for intelligent calf raising. When a calf enters the feeding area, the 3D visual module measures its body length, width, and height while the load cell sensor detects its weight. The data is transmitted via cable to the data collection server. In addition to displaying the server's data, the system also introduces milk consumption information from the automated feeder. The equipment gains intelligence from Internet of Things (IoT), information and communication technology, and image recognition technology, while data analysis and expert raising experience enables it to communicate with other equipment or humans. The administrator needs only to check the farm network to learn about calf growth information on the main server.

2. System architecture

Figure 1 is a diagram of the feeding management system. The 3D visual module shall be set up above the automated calf feeder, and the load cell sensor module installed below. The measurement range is detected through the 3D visual module and image processing, while calf number within the range is determined through the kurtosis trend that the load cell sensor module returns. Considering the transmission distance and computing speed, the captured image and weight sensing data are first sent to the calf zone data collection computer. The feeding system then receives data returned from the calf zone while capturing feeding

information that is sent by the automated feeder to the feeder server and uploaded to the Calf Guide system.
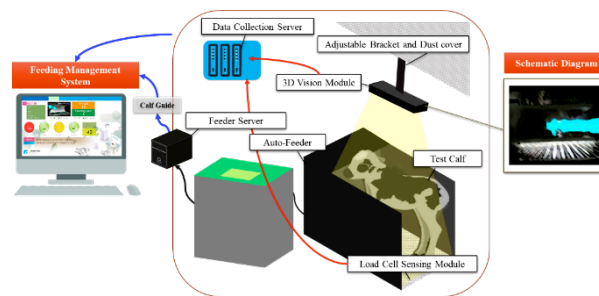

Figure.1. Diagram of the feeding management system

The 3D camera used in this study captures 2D and 3D images simultaneously. Its detection range is 0.5m-4.5m and resolution is 1920*1080. The weight sensor is the load cell force sensor and the interfaced Calf Guide system is from Holm-Laue. Detailed hardware structure includes: 3D camera, load cell sensor module, automated feeder, extruded aluminum frame, data collection server, feeder server, and feeder management system.

3. System process and implementation

This study applies image recognition technology to body size measurement, automatically measuring calf body length, width, height, and weight when it enters the feeding zone. To avoid disturbing the traffic flow around the feeding zone and to minimize detection errors caused by personnel at work, the 3D visual module is installed directly above the automated feeder, while the load cell sensor module is installed beneath the feeder. Detailed measurement process and environment are shown in Figures 2 and 3.
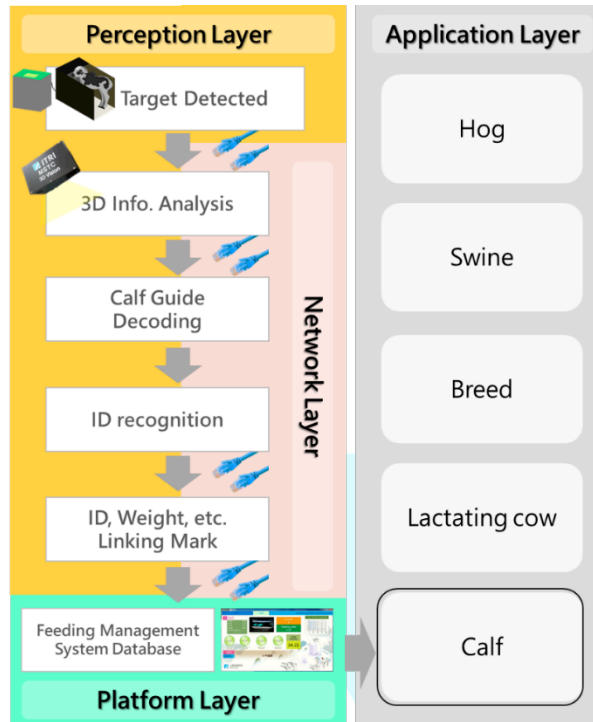
Figure.2. Measurement process chart
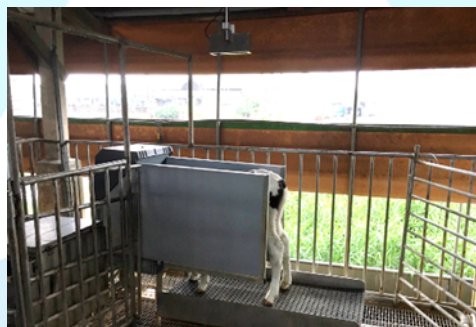
Figure.3. Measurement environment

The projection range of the 3D visual module is shown in Figure 4. To determine accurate calf body size data, complete 3D point cloud information for the calf must be obtained. If point cloud information is based on the 3D camera coordinates (plane ZcYc), the measurement will be easily affected by the calf position and size, and the measurement algorithm threshold will be hard to determine. If the reference coordinates are changed to the floor (plane ZgYg), the relation between calves and the floor will be simpler, and the measurement results will be more reliable.

The transition matrix can be calculated by using the known relative relation-ships between the 3D camera and the floor. Then, the 3D point cloud information can be converted

to the floor coordinates system via the transition matrix, and the subsequent calf appearance measurement is performed.

Figure.4. Actual projection range of the 3D visual module
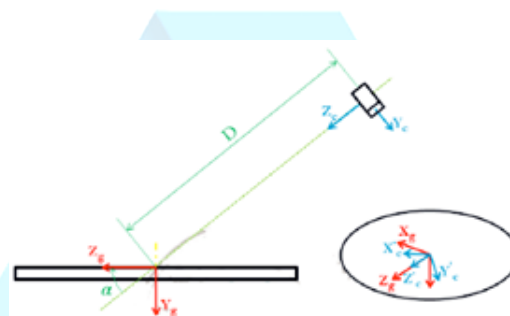
Figure.5. Transformation diagram for the 3D camera and the floor coordinates

Figure 5 is a transformation diagram for the 3D camera and the floor coordinates. Values for α and D must be determined in order to employ the transition matrix. The D value can be directly measured the distance from the 3D camera to the floor center. The α value is more complex. First the floor plane with no calves present must be recorded to obtain its point cloud information. The normal vector of the plane $\vec{N}$ is then calculated with the point cloud information and used for determining α, as shown in Figure 6.

Figure.6. Relationship between the alpha value of the transformation matrix and the plane normal vector

The 3D camera coordinates system is shifted to distance D so that the origin is at the center of the floor plane. Then, it is rotated α degrees so that the Yc axis coincides with the Yg axis. After translation and rotation, Xg, Yg, and Zg are the floor co-ordinates as shown in Figure 5. The mathematical equation is as below:

$$\begin{bmatrix} X_g \\ X_g \\ X_g \\ 1 \end{bmatrix} = \begin{bmatrix} 1 & 0 & 0 & 1 \\ 0 & cos\,\alpha & sin\,\alpha & 0 \\ 0 & -sin\,\alpha & cos\,\alpha & 0 \\ 0 & 0 & 0 & 0 \end{bmatrix} \begin{bmatrix} 1 & 0 & 0 & 1 \\ 0 & 1 & 0 & 0 \\ 0 & 0 & 1 & -D \\ 0 & 0 & 0 & 1 \end{bmatrix} \begin{bmatrix} X_c \\ X_c \\ X_c \\ 1 \end{bmatrix} \qquad (1)$$

A plane equation can be considered as an infinite plane in a 3D space. Within a 3D x-y-z coordinate system, a plane can be defined as a solution set to an algebraic equation. A plane in three-dimensional space has the equation:

$$f(x_i, y_i, z_i) = Ax_i + By_i + Cz_i + D = 0 \qquad (2)$$

Where (x_i, y_i, z_i) is the 3D point cloud coordinates that correspond to the floor plane. A, B, C, and D are the coefficients to the geometric algebra plane equation, of which (A, B, C) is the normal vector. To obtain the point cloud of the floor plane, the 3D camera records 3D point cloud information of the floor plane with no calves present. The floor plane range is then selected with a paintbrush, as shown in Figure 7.
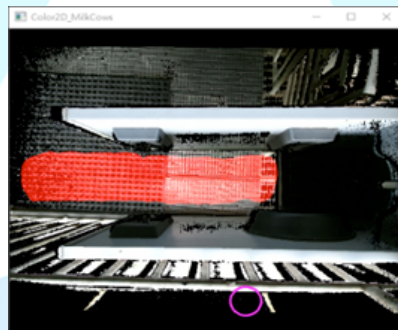
Figure.7. The floor plane range is then selected with a paintbrush

To estimate the normal vector for the floor plane, the predefined floor plane 3D point cloud information is used to find k-nearest neighbor point clouds and perform principal component analysis (PCA) [1]. Principal Component Analysis (PCA) is a dimension-reduction tool that can be used to reduce a large set of variables to a small set that still contains most of the information in the large set. Because the eigenvectors of the covariance matrix are orthogonal to each other, they can be used to reorient the data to the axes represented by the principal components. And, the eigenvector that corresponds to the smallest eigenvalue is the normal vector. Specifically, each point Pi is arranged to give the below CM.

$$CM = \frac{1}{k}\sum_{i=1}^{k}(p_i - \bar{p}) * (p_i - \bar{p})^T \, , CM \cdot \vec{V_j} = \lambda \cdot \vec{V_j} \qquad (3)$$

Where, k is the number of floor point clouds (Pi), $\bar{p}$ is the center point of the k-nearest neighbor points, λ_j and $\vec{V_j}$ are the j-th eigenvalue and eigenvector for CM, respectively.

Since the calf measurements are restricted to a specific zone within the 3D camera range, this zone is named the region of interest (ROI). In Figure 8, for example, the zone framed in purple is established as the ROI. Then, impossible targets can be preliminarily filtered out and calculation time is decreased.
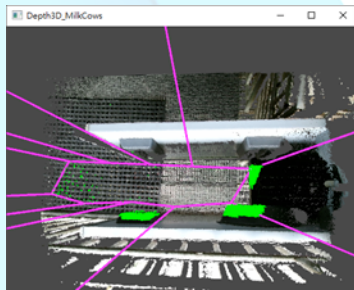
Figure.8. The zone framed in purple area is established as the ROI

When a calf enters the ROI and the 3D point cloud is higher than the floor plane (with coordinates converted to the floor coordinate system), its point cloud is displayed in green. Figure 9 shows the segmented point cloud. The green point cloud includes the calf and feeding zone flaps, so the calf point cloud must be cleanly segmented to avoid affecting subsequent body shape analysis.
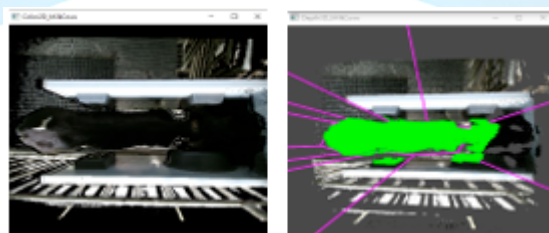
Figure.9. The segmented point cloud

To obtain a pure calf point cloud, a background subtraction algorithm is employed with depth information to give a foreground depth image [2]. The rationale is to use the stationary depth scene as the background image model, subtracting the background depth image from

the current depth image information captured by the 3D camera to obtain a foreground block. If the difference value is greater than preset threshold, it can be analyzed that the image captured by camera is different from the background image. And, it indicates that there might be a moving object in the image. If the difference value is less than the preset threshold, it can be analyzed that there is no change in the image.

$$f_s(x,y) = \begin{cases} D_s(x,y), & |D_s(x,y) - B(x,y)| > TH \\ 0, & Otherwise \end{cases} \quad (4)$$

In which $B(x,y)$ is the preset background image model as shown in Figure 10, and $D_s(x,y)$ is the s-th depth image captured by the 3D camera as shown in Figure 11. After subtraction, the depth value retained if the depth difference value is larger than the preset threshold TH. Otherwise, the value is set to 0. After background subtraction with depth information, the pure calf 3D point cloud is shown in Figure 12.
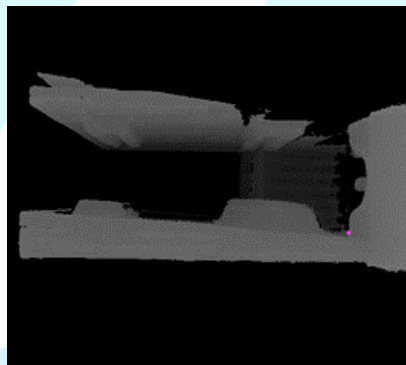

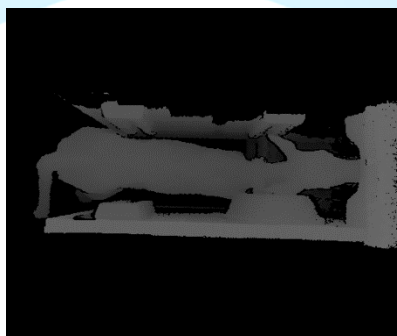Figure.10. The preset background image model

Figure.11. Depth image which is captured by the 3D camera
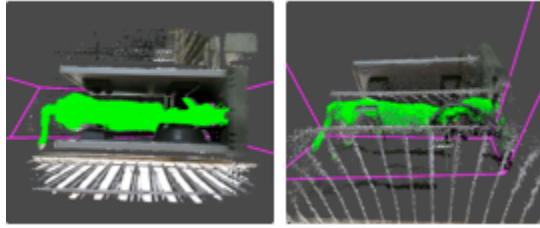
Figure.12 The clean calf 3D point cloud after background subtraction with depth information

Once the pure calf 3D point cloud information is obtained, the actual X-Y-Z axis point cloud is converted through projection towards X-Z and X-Y directions to simplify the complexity of cow body measurement. The X-Z projection is used to calculate the calf's maximum height, while the X-Y projection is used to calculate calf body length and width.
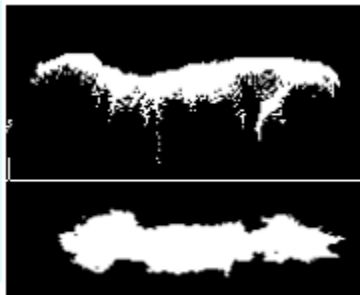
Figure.13. The actual X-Y-Z axis point cloud is converted through projection towards X-Z (above) and the X-Y projection result (below)

Regarding the load cell sensor module, when a calf enters the milk-drinking area, the sensor reads automatically, utilizing kurtosis determination mechanisms to confirm if there is a calf entering. If only a calf enters the area, the body length, width, and height information measured by the 3D visual module is received and recorded. On the other hand, the Calf guide system info page is simultaneously started, and milk drinking amount determination is decoded in real time. The system automatically retrieves the latest milk consumption information, and the calf that is currently drinking are identified. Finally, the calf identity, weight, and measurement information are labeled, linked together, and written in the database.

4. Data analysis

The study started on 2018/09/28 and ended on 2019/02/01. A total of 145 data sets were collected. After discarding invalid samples, the calves were divided by milk consumption into three groups. Group 1 consisted of calves which drank 2 liters or less milk, sample size was 41; group 2 consisted of those drinking 2.1 to 4 liters, sample size was 35; and group 3 were

those drinking 4.1 liters and more, of sample size 34. The body lengths, widths, heights, and weights of each group were recorded separately.

Table 1. Correlation coefficient between body length, width, height and weight

	(Length)	(Width)	(Height)
Group 1	0.818778	0.671578	0.747445
Group 2	0.800891	0.620181	0.881510
Group 3	0.717194	0.764294	0.766822

Based on the body length, width, and height variance to body weight distribution diagrams for groups 1 to 3, we infer that the data are positively correlated to body weight. The calculated correlation coefficients for each group are listed in Table 1. To learn more about the correlation between body length, width, and height and weight, regression analysis [3] was used to create a correlation model, with body weight defined as dependent variable y, and body length, width, and height as x1, x2, and x3, respectively. The least square method [4] was used to determine regression coefficients B0, B1, B2, and B3, with the corresponding model fitting results as below. The F-test, which the correlation model is suitable when P-value<0.05 [5], was used to check overall model appropriateness. The multiple R-squared value in the table, which is the coefficient of determination (R2), was further examined to verify the model's explanatory power. In group 1, for instance, the three variables body length, body width, and body height have 80.25% explanatory power over body weight, while in group 2 the body width Pr(>|t|) to body weight is 0.3706 (more than 0.05), meaning that this variable is not suitable for incorporating into the model. Thus for group 2 only the body length and height are included in the correlation equation written into the feeding management system that is based on data analysis.

Table 2. Model matching result (Group 1)

Group 1	Estimate	Std. Error	t value	Pr(>|t|)
B0	-85.25047	11.1677	-7.634	4.13e-09 ***
B1(Length)	0.42887	0.07934	5.405	4.01e-06 ***
B2(Width)	0.83387	0.28227	2.954	0.00542 **
B3(Height)	0.60952	0.17369	3.509	0.00120**

Residual standard error: 2.403 on 37 degrees of freedom
Multiple R-squared: 0.8173, Adjusted R-squared: 0.8025
F-statistic: 55.16 on 3 and 37 DF, p-value: 9.926e-14

Table 3. Model matching result (Group 2)

Group 2	Estimate	Std. Error	t value	Pr(>|t|)
B0	-107.7506	11.4188	-9.436	9.19e-11 ***
B1(Length)	0.4121	0.1239	3.324	0.00223 **
B2(Height)	1.1543	0.1891	6.103	8.06e-07 ***

Residual standard error: 2.403 on 37 degrees of freedom
Multiple R-squared: 0.8173, Adjusted R-squared: 0.8025
F-statistic: 55.16 on 3 and 37 DF, p-value: 9.926e-14

12

Table 4. Model matching result (Group 3)

Group 3	Estimate	Std. Error	t value	Pr(>|t|)
B0	-90.8868	13.0971	-6.939	1.05e-07 ***
B1(Length)	0.2330	0.1080	2.157	0.03914 *
B2(Width)	1.6338	0.4501	3.630	0.00104 **
B3(Height)	0.7034	0.2072	3.395	0.00195 **

Residual standard error: 2.643 on 30 degrees of freedom
Multiple R-squared: 0.7821, Adjusted R-squared: 0.7603
F-statistic: 35.89 on 3 and 30 DF, p-value: 4.734e-10

5. Result and discussion

This study combines the concept of IoT to offer a feeding management system that can be applied to dairy farming. A 3D image sensor collect calf body shape information, a weight sensor obtains calf body weight, and data analysis is utilized to create correlation models for calves with different milk consumption volumes. Based on the models, calf requirements can be predicted. Lastly, interaction in both ways between humans and equipment and between equipment sets can be realized through IoT structures. Figure 14 is the user interface of the feeding management system that developed in this study. When a calf enters the feeding area, the system fits it with the appropriate model and predicts its weight according to the calf's total milk consumption amount in the prior day. Based on predictive values and actual values within an interval, the system also provides calf health status description and suggestions, such as: Healthy, activities should be noted, growing rapidly, maybe diarrhea, need more than 2 liters milk, or increase to 6 liters milk.

Figure.14. Feeding management system

The feeding management system is implemented and proved that it can help farm administrators detect abnormal calves earlier and adjust raising methods according to system recommendations. However, apart from calf growth management, a feeding management system used in dairy farming must include additional measurements and incorporate lactating cow growth management to have extended system applicability as well as complete control over cow growth traceability. Therefore, future work shall focus on data collection and

analysis for lactating cows. Besides integrating the 3D image sensor, gas sensor, and load cell sensor, a thermal image sensor will also be added to obtain overall data on lactating cows' growth data such as energy, body shape, and body temperature, resulting in a comprehensive feeding management system.

References

1. Alexa, M. & Adamson, A. (2004). On normals and projection operators for surfaces defined by point sets, *in Proceedings of Symposium on Point-Based Graphics 04*, 149–155.

2. Collins, R. & Lipton, A. & Kanade, T. (2000). A system for video surveillance and monitoring, The Robotics Institute, Carnegie Mellon University, CMU-RI-TR-00-12.

3. https://www.statisticshowto.datasciencecentral.com/probability-and-statistics/regression-analysis/

4. Miller, S. J. (2006). The method of least squares, Mathematics Department, Brown University.

5. https://www.statisticshowto.datasciencecentral.com/probability-and-statistics/hypothesis-testing/f-test/

Tool Path Optimization of CNC Hand-drawn Batik Machine using Master-Slave Genetic Algorithm

Hafidz Ridho[a], Andi Sudiarso[a], R.J. Kuo[b]

[a]Department of Mechanical and Industrial Engineering, Universitas Gadjah Mada, Indonesia

[b]Department of Industrial Engineering, National Taiwan University of Science and Technology, Taiwan

E-mail address: [a]hafidzridho@mail.ugm.ac.id, a.sudiarso@ugm.ac.id, [b]rjkuo@mail.ntust.edu.tw

Abstract

Automation in the batik industry is one of the solutions to anticipate the decreasing number of batik artisans in Indonesia. Several studies related to batik process automation are mainly focused on the quality of finished batik products. Another challenge is to optimize the production time of the CNC hand-drawn batik machine by determining the sequence of batik making process in order to get the shortest tool path. Batik process can be considered as an open arc routing problem, where the optimization focuses on arcs instead of a single node and every arc has two nodes that represent entry and exit points. This study intends to apply a genetic algorithm (GA) to find the best operation sequence by modeling batik process as an open arc routing problem. Chromosome mechanism named master-slave chromosome is used where master chromosome represents sequence of the main arcs and slave chromosome represents entry point of the corresponding arcs. The optimization result shows that master-slave GA can get shorter distance compared to operating sequence manually performed by batik artisan. The results also show that GA significantly has better performance compared to other classical algorithms namely Sine-cosine Algorithm (SCA) and Particle Swarm Optimization (PSO) in terms of obtaining global optimum, even though it needs more computational times to complete the iteration.

Keywords: Batik, Open arc routing problem, Optimization, Genetic algorithm.

1. Introduction

Batik is one of Indonesia's cultural icons and has become a national identity known to the world. Indonesian Batik has been designated as a Humanitarian Heritage for Oral and Non-Cultural Culture by UNESCO (United National Educational, Scientific and Cultural Organization) since October 2, 2009. Reported from the Indonesian Ministry of Industry website, the Indonesian batik industry is considered to have mastered the world market based on the achievements of the export value of batik and batik products in 2017 which reached USD 58.46 million (Indonesian Ministry of Industry, 2019).

In its development, despite being in the middle of a potential world apparel market opportunity, the batik industry in Indonesia still has various problems. One of the problems experienced by the national batik industry was the lack of batik workers, especially hand-drawn batik artisans (Kusumawardani, 2018). Several studies have been carried out to fill the void generation of hand-drawn batik artisans through the automation system, such as automatic batik machines for stamped batik (Wibisono *et al.*, 2012) and computer numerical control (CNC) based hand-drawn batik (Kusumawardani, 2018). The results of the batik process using the automatic batik machine developed by Kusumawardani (2018) shows that the automatic batik machine requires shorter production time than the manual batik process and is able to produce batik with a similar quality compared to manually hand-drawn batik process.

The focus of research conducted by Kusumawardani (2018) is to replicate the manual batik process carried out by hand-drawn batik artisans. Another challenge is how to get the optimal process in terms of production time. The total production time using a CNC machine consists of travel time, tool switch time, and cutting time (Qudeiri *et al.*, 2006). Since the parameters on the productive movement affects the product quality, this study will more focus on minimizing travel time by finding the best sequence of operations in order to get the shortest tool path. The optimization can be done by formulating the problem as the open arc routing problem and solve it with some metaheuristics. Although it may not get optimal results, it is still acceptable because they are considered to have approached near-optimal results.

2. Literature review

Several studies have been carried out to optimize the CNC process in terms of minimizing travel time using various metaheuristic algorithms. Based on the review that has been carried out, the case of CNC has quite a lot of variations, in terms of the number of cutting tools, machining level, and arc profile. The classification of CNC cases that used as a guide to the literature review in this study is illustrated in Figure 1.

In the case of closed arc, single level, and single tool, Ancau (2009) tried to minimize the

total distance of the spindle path in the PCB drilling process using the heuristic method. The optimum global route search is done by deterministic methods. In contrast to Ancau (2009), Adam, *et al.* (2010) used a metaheuristic method with the particle swarm optimization (PSO) algorithm to optimize a previous study conducted by Zhu (2006) regarding to the PCB drilling optimization. Narooei, *et al.* (2014) tried to solve the CNC drilling case using the ant colony optimization (ACO) algorithm. The ACO algorithm was also used by Rodriguez, *et al.* (2012) and Ross, *et al.* (2012) to solve closed arc, single level, and single tool cases. Research conducted by Rodriguez, *et al.* (2012) tried to develop the ACO algorithm to get the shortest tool path in the drilling process using a CNC machine by doing iterations in parallel. Ants are first divided into groups, then iterations are carried out in parallel with different processors in each group. The same method was also carried out by Ross, *et al.* (2012) to minimize the tool path by using parallel-ACO. The conclusion obtained by Ross, *et al.* (2012) was the addition of processors can increase processing time.
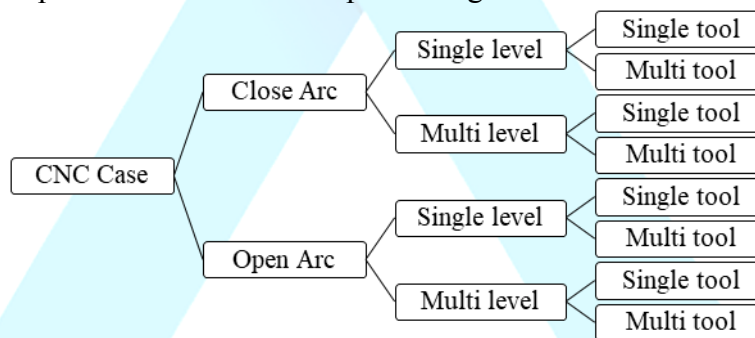

Figure 1: CNC cases classification

Balakhrisnan and Savaranan (2017) solved the tool path optimization problem in the CNC drilling process by modeling the movement of the cutting tool as a TSP case and solved it using genetic algorithm (GA). GA was also used by Shipacheva, *et al.* (2017) to minimize the tool path in the plate cutting process. The hybrid algorithm between GA and the Taguchi method has been developed by Al-Janan and Liu (2016) to solve the same problem in a study conducted by Lim, *et al.* (2014). The stages of this method are evaluating the machining path and formulating it as a TSP case, finding alternative routes that are carried out using GA and then applying to the Taguchi method to find the best combination based on the design of experiment. The conclusion obtained from this study was that the HTGA method is judged to be more adaptive and faster to obtain convergence speed compared to previous studies conducted by Lim, *et al.* (2014). The novelty raised in this study is the combination of the Taguchi and GA methods that have never been done before.

In the case of closed arc, multi-level, and single tool, Abdullah, *et al.* (2017) tried to optimize the tool path in three-dimensional machining of work pieces using a CNC milling machine. The parallel-ACO algorithm is used in this study to determine the sequence of processes that produce the shortest tool path. Qudeiri, *et al.* (2013) also developed

17

formulations for solving closed arc, multi-level, and single tool cases using GA. The results of the optimization showed that the shortest route can be achieved by completing a sequence of operations at one level until it is finished and then moving to the next level.

In the case of closed arc, multi-level, and multi-tools, research conducted by Qudeiri, *et al.* (2013) tried to develop a formulation in a previous study conducted by Qudeiri, *et al.* (2006) by adding a multi-tool case to the work order optimization problem in a multi-level CNC milling process. Optimization is done using GAs. The novelty raised in this study is the formulation for a combination of multi-level and multi-tools, which is complex enough to group the sequence of processes based on the cutting tools used and avoid unwanted machining when cutting tools move to different levels.

The majority of research aimed at minimizing the tool path takes drilling cases as a problem to be solved where the machining process can be classified as closed arc cases. Not much research has discussed the optimization of CNC in the case of open arc. The case of the open arc explained as: if the entry point and exit point of the productive movement are at different points. One example of an open arc case is CNC laser cutting. A study to minimize the tool path in the laser engraving process using the hybrid-coded GA can be seen on Chen and Zhong (2002). There are two chromosomes used, namely the slave chromosome and the master chromosome. The master chromosome represents the productive movement of the cutting tool, while the slave chromosome represents the entry and exit points that follow the master chromosome. This laser engrave case is similar to the case of CNC hand-drawn batik, where productive movements tend to form curves and have different entry and exit points.

Based on the literature review that has been carried out on several publications related to the optimization of the CNC process, this research design can be mapped into the case of open arc, single level, and single tools. Since the case study quite similar with Chen and Zhong (2002), this study also uses GA with similar master-slave chromosome mechanism to find the near-optimal tool path sequence. Sine-Cosine algorithm, firstly proposed by Mirjalili (2016) and PSO will also be used as comparison to GA.

3. Research Ojectives

3.1 Digitalization of traditional Indonesian batik pattern, namely Megamendung, in the form of vector designs and G-Code that are ready to be produced using CNC Hand-drawn batik machines.

3.2 Optimize the operating sequence to get the shortest tool path using master-slave GA so the production time can be shortened.

4. Methods

4.1 Batik Digitalization

The object analyzed in this study is the manual process of Batik Megamendung which is crafted by batik craftsman from Giriloyo, Bantul, Special Region of Yogyakarta, Indonesia. Traditionally, batik is crafted manually by hand. In order to be processed in CNC Batik Machine that has been developed by Kusumawardani (2018), digitalization process is needed. The digitalization also provides the coordinate of each node so optimization can be done based on the distance matrix. The steps of digitalization process are explained as follows:

1) *Batik process documentation*. Documentation is carried out using a digital camera to record the manual batik process crafted by batik artisan from beginning to end.
2) *Digitalization process*. Digitalization is needed to translate batik patterns that are done manually into vector format using bezier tool feature in the image processing software namely Inkscape.
3) *G-Code generation*. G-Code can be generated using the Path to G-code feature in the G-code tools submenu in the Extensions section. The line in the image will be identified as the batik path, while the tool movement from the finished batik point to the next batik point will be generated automatically.
4) *G-Code validation*. Software Mach3-Mill is used to validate the finished G-Code by simulating the tool path.

Figure 2 shows the digitalization result of Megamendung Batik pattern that will be optimized in this study. Totally there are 466 main segments.
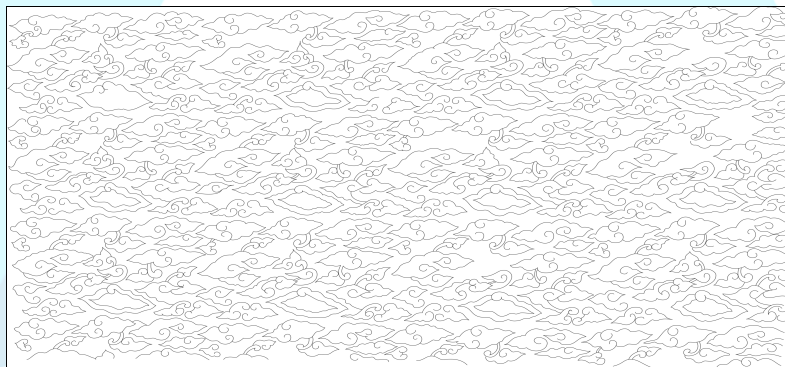

Figure 2: Digitalization result of Megamendung Batik Pattern

4.2 Problem formulation

Open arc routing problem is considered as NP-hard problem to optimize operation sequence between set of segments where each segment has different start and finish position. Figure 3 explains the difference between TSP, capacitated arc routing problem, and open arc routing problem.
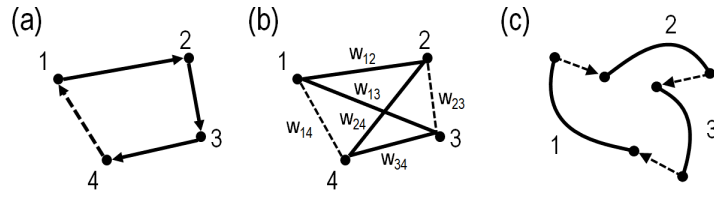
Figure 3: Routing problem comparison. (a) TSP. (b) Capacitated arc routing problem. (c) Open arc routing problem

Let $S = \{s1, s2, ..., sn\}$ is a collection of a number of "n" main segments. The total tool path travel distance (*TL*) can be calculated from the sum between the total distance of the main segment (*TS*) and the total distance of the connecting arc (*TC*). Equation (1) shows the calculation of the total distance of the whole. Because TS is a batik pattern that must be present and can't be reduced, the objective function for the optimization case in this study can be simplified according to (2) as follows:

$$TL = TS + TC \tag{1}$$

$$min\ TC = \textstyle\sum_{i,j \in S} x_{ij} d_{x_{i_k j_l}} \tag{2}$$

where $x_{i_k j_l}$ is decision variable of path selection from segment i leaving from point k to segment j entering from point l and $d_{x_{i_k j_l}}$ is the distance related to that decision variable.

Distance of the non-productive movement (*d*) is calculated using the Euclidean distance principle. The distance of the non-productive movement (*d*) is explained by (3):

$$d = \sqrt{(x_{i+1} - x_i)^2 + (y_{i+1} - y_i)^2} \tag{3}$$

where x_i and y_i are the end point coordinates of the segments that have already been processed, while x_{i+1} and y_{i+1} are the start point coordinates of the next segment to be processed. The coordinates of the end point and start point are obtained from the coordinates contained in the G-code. The constraints are formulated as follows:

$$\textstyle\sum_{i=1}^{n} x_{ij} \leq 1 \qquad\qquad j = 1, ..., n \tag{4}$$

$$\textstyle\sum_{j=1}^{n} x_{ij} \leq 1 \qquad\qquad i = 1, ..., n \tag{5}$$

$$\textstyle\sum_{i=1}^{n} x_{im} + \textstyle\sum_{j=1}^{n} x_{mj} = 1 \qquad\qquad m = 1, ..., n \tag{6}$$

$$u_i - u_j + n x_{ij} \leq n - 1 \qquad\qquad i, j = 2, ..., n \tag{7}$$

$$x_{ij} \in \{0,1\} \tag{8}$$

Constraints (4) and (5) express that each node can be visited up to once. Constraint (6) forces the decision variable to choose different entry points and exit points at the same main segment for the next sequence, as explained by (2). For each main segment S, if point k is

20

already chosen as an entry point, point l is forced to become the exit point for the next sequence, and point k can not be chosen anymore. Constraint (7) expresses that the solution has a single cycle instead of a set of cycles that covers all the cities.

4.3 Master-slave Genetic Algorithm

GA is known for its superiority to solve discrete problems. Several terms are commonly used in GA and the parameter used in this study are explained as follows:

1) *Chromosome*. A chromosome is an individual consisting of genes that represent alternative solutions. A collection of chromosomes is called a population. In the open arc routing problem, there are two sets of chromosome within each individual that represent main segment and entry point of the segment. This representation is known as master-slave chromosome Chen and Zhong (2002), and illustrated by Figure 4.
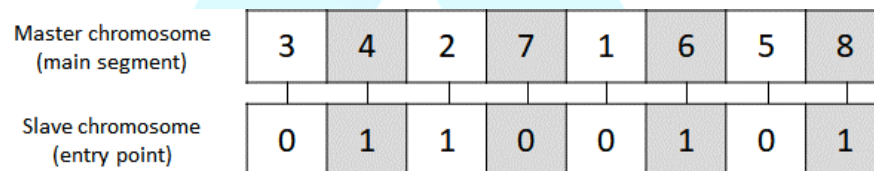

Figure 4: Master-slave chromosome (Chen and Zhong, 2002)

2) *Fitness*. Fitness is a unit that measures how good the quality of a chromosome is. The fitness value of one chromosome will affect the chances of choosing the chromosome as parents and the chances of survival of the chromosome in the next generation. Equation (2) is used as fitness function in this study.

3) *Elitism*. Elitism aims to maintain the best chromosomes of one generation to continue appearing in the next generation. Elitism can be chosen by copying the best chromosomes as a new individual.

4) *Roulette wheel*. The roulette wheel is used for chromosome selection operations. The fitness of each chromosome is sorted from the best then made a cumulative distribution based on that order. Random numbers from 0-1 are then generated to select chromosomes by adjusting the cumulative distribution values. Chromosomes that have better fitness will have a greater chance of being selected.

5) *Crossover*. Crossover is a process of exchanging genes between one and another chromosomes to produce a new chromosome. Crossover scheme that used in this study is single-point partially mapped crossover (Santoso and Willy, 2011). For the selected parents, cutting point is randomly chosen to divide the chromosome into two sets of genes. Then, exchange the genes that has no conflicts and then change

the conflicted value based on mapping. Figure 5 explains the crossover scheme used in this study.

Figure 5:   Single-point partially mapped crossover

6) *Mutation*. Mutation is the process of exchanging genes within chromosome. The chromosomes and genes that going to be mutatied are selected based on random numbers. In this study, two stages of mutation is applied. First stage is to swap two random genes in both master and slave chromosomes within selected individual. The next stage is to mutate the selected gene in slave chromosome. All selection is performed with random selection. Figure 6 ilustrates the two stage mutation used in this study.

Figure 6: Two stage mutation. (*a*) First stage: exchange genes within individual.
(*b*) Second stage: mutation on slave chromosome

4.4 Experimental design

There are several parameters that need to be determined in order to get the best result. Parameters used in GA are: (1) population size, (2) crossover rate, (3) mutation rate, and (4) maximum iteration number. Different values for each of parameters are tested with combination to get the best result. Table 1 explains the sets of values that are going to be tested. By combining all the sets, totally there are 27 scenarios that are going to be tested.

Table 1: Sets of GA Parameter.

Parameter	Value 1	Value 2	Value 3
Pop size	30	40	50
Crossover rate	0.7	0.8	0.9
Mutation rate	0.1	0.2	0.3

The optimization is carried out using Python language on a computer with Intel® Core™

i7-6700 CPU @3.40GHz (8CPUs) and 20,480 MB RAM. For testing purpose, this study uses 20 first instances from real data and uses 100 iterations. Each scenario is replicated 30 times to get the average value of the global best. The experimental results are illustrated in Table 2. From Table 2, it can be concluded that the best result can be found on scenario 6, whose population size is set to 50, crossover rate is set to 0.8, and mutation rate is set to 0.3.

Table 2: Parameter Tuning Results

Scenario	Pop Size	Crossover Rate	Mutation Rate	Global Best Mean	Global Best Rank	Scenario	Pop Size	Crossover Rate	Mutation Rate	Global Best Mean	Global Best Rank
1	50	0.9	0.1	217.9	13	15	40	0.8	0.3	212.41	9
2	50	0.9	0.2	200.7	5	16	40	0.7	0.1	231.93	23
3	50	0.9	0.3	195.55	2	17	40	0.7	0.2	212.73	10
4	50	0.8	0.1	204.72	7	18	40	0.7	0.3	223.38	18
5	50	0.8	0.2	195.58	3	19	30	0.9	0.1	230.73	22
6*	50*	0.8*	0.3*	192.37*	1*	20	30	0.9	0.2	240.02	26
7	50	0.7	0.1	228.58	19	21	30	0.9	0.3	234.03	25
8	50	0.7	0.2	199.3	4	22	30	0.8	0.1	228.94	20
9	50	0.7	0.3	201.77	6	23	30	0.8	0.2	233.48	24
10	40	0.9	0.1	213.63	11	24	30	0.8	0.3	218.53	14
11	40	0.9	0.2	217.63	12	25	30	0.7	0.1	241.15	27
12	40	0.9	0.3	207.27	8	26	30	0.7	0.2	230.32	21
13	40	0.8	0.1	218.79	15	27	30	0.7	0.3	219.44	16
14	40	0.8	0.2	221.54	17						

The parameter used in SCA is $a = 2$, and those for PSO are $c_1 = 0.5$, $c_2 = 0.5$, and $w = 0.95$. The solution representation of PSO and SCA is similar with the master-slave chromosome in GA, where each particle has two sets of solutions that represent the main segment and entry point. For each particle, those two sets of solution are updated individually based on their personal best or current global best.

Since PSO and SCA are naturally used for continuous optimization, discretization technique is needed. Random number between 0 to 1 is generated in the size of *dimension*particle* for initial value. The discretization process is carried out by sorting the decimal value for each particle solution, then find the corresponding index for each random value relative to original particle solution (Santoso and Willy, 2011). Discretization process is visualized by Figure 7.

$$x_t = \begin{bmatrix} 0.13 & 0.56 & 0.24 & 0.93 \\ 0.85 & 0.52 & 0.54 & 0.32 \\ 0.11 & 0.76 & 0.03 & 0.65 \end{bmatrix}$$

$$x_{sort} = \begin{bmatrix} 0.13 & 0.24 & 0.56 & 0.93 \\ 0.32 & 0.52 & 0.54 & 0.85 \\ 0.03 & 0.11 & 0.65 & 0.76 \end{bmatrix} \qquad x_{discrete} = \begin{bmatrix} 1 & 3 & 2 & 4 \\ 4 & 2 & 3 & 1 \\ 3 & 1 & 4 & 2 \end{bmatrix}$$

Figure 7: Discretization technique

5. Results and Discussion

The manual sequence performed by batik craftsman is included as one of the chromosome within a population. The manual sequence already gives a good result, since the craftsman naturally chooses the nearest pattern from previous pattern that already drawn. By including the manual sequence as a starting point, the optimization surely can give the better result compared to the manual one.

Population size used in this study is 50. Since the gene length is quite high (466 segments with 932 nodes), the number of iterations is set to 100,000 to ensure that the optimization convergence can be achieved. The optimization results are explained in Table 3, and the convergence graph is explained in Figure 8, while Table 4 shows the statistical analysis to compare the results from GA, PSO, and SCA.

Table 3: Optimization Results

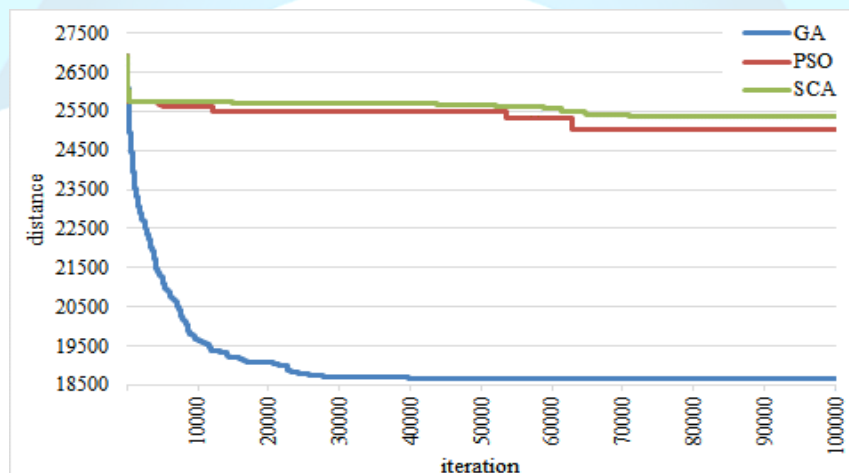|	Manual Process	GA*	PSO	SCA
Min	26,905.06	**18,660.25**	25,049.24	25,348.43
Max		**19,427.56**	25,796,02	26,167.11
Average		**19,069.95**	25,351.51	25,773.56
Std. deviation		**188.53**	175.71	180.85

Figure 8: Convergence graph

24

From Figure 8 it can be seen that GA begin to slowly converge at iteration 40,000, while PSO and SCA are tend to be trapped on the local minimum. With 100,000 iterations, the minimum distance obtained by using GA is 18,660.25 and improved 31% better compared to the manual sequence, which is 26,905.06.

The statistical analysis shown in Table 4 reveals that with significance level $\alpha = 0.05$, GA is significantly different compared to PSO and SCA. GA outperforms PSO and SCA because its nature is to solve discrete problem, while PSO and SCA is more suitable to solve continuous problem. With the high dimensions, PSO and SCA are tend to be trapped on the local minimum because the updating process on the set of continuous values, that represents the sequence, will result in a totally different sequence from the previous solution.

Table 4: Statistical analysis

$\alpha = 0.05$		GA	PSO	SCA
Test type	GA	-	t-test	t-test
	PSO		-	t-test
	SCA			-
P-value	GA	-	7.41877	7.93794
	PSO		-	5.49761
	SCA			-
Decision*	GA	-	1	1
	PSO		-	1
	SCA			-

"0" means there is no significant difference between paired samples, while "1" means there is a significant difference.

The computational time is explained in Table 5. Table 5 shows that computational time of GA is significantly longer than PSO and SCA. The most time-consuming aspect of the algorithm is the calculation of objective function. Since the number of particles of PSO and SCA is fixed for each iteration, the number of calculations of the objective function is also fixed. While for GA, the mating algorithm will generate a new population that needs to be evaluated for the natural selection process so the computational time is significantly increased. Even though GA needs more computational time to complete 100,000 iterations, it still has better performance because the optimal result from PSO (25,049.24) can be obtained by GA with only 390 iterations and only needs 0.07 hours while the optimal result from SCA (25,348.43) can be obtained with 335 iterations and only needs 0.06 hours.

Table 5: Computational time (hours)

	GA	PSO	SCA
Min	20.45	4.81	**3.96**
Max	25.85	6.29	**4.33**
Average	22.08	5.13	**4.09**
Std. deviation	1.51	0.37	**0.13**

25

6. Conlcusions

In this paper, we presented an implementation of master-slave chromosom on GA, to optimize CNC hand-drawn batik process. The production of batik with CNC hand-drawn batik machine already performs faster than manual process with a similar quality. This paper provided a solution to improve the process with even more efficient way by finding optimal operation sequence so the tool path travel distance can be reduced. This tool path was formulated as an application of the open arc routing problem. The application of master-slave GA and open arc routing problem can be applied to any similar problem, such as CNC milling, CNC laser cutting, and fused deposition modelling on 3D-Printing. Compared to PSO and SCA, GA significantly has better performance even though it needs more computational times to complete the iteration.

References

1. Indonesian Ministry of Industry (2019). Tembus Pasar Jepang Hingga Eropa, Ekspor Batik Nasional Lampaui USD 58 Juta. Retreived from http://www.kemenperin.go.id/artikel/ 19253/Tembus-Pasar-Jepang-Hingga-Eropa,-Ekspor-Batik-Nasional-Lampaui-USD-58-J uta.

2. Kusumawardani, R. (2018). *Perancangan Motif dan Produksi* Batik *Tulis pada Mesin CNC* Batik *Tulis untuk Meminimalkan Waktu Pem*batik*an*, Thesis Magister of Industrial Engineering Universitas Gadjah Mada, Yogyakarta.

3. Wibisono, M.A., Dharma, I.G.B.B., Suwastono, and A., Imani, M.A., (2012). Integrasi Desain dan Manufaktur Batik Cap. *Jurnal Ilmu Pengetahuan dan Teknologi Tepat Guna Universitas Gadjah Mada*, 1(2), 73-812.

4. Qudeiri, J.E.A., Raid, M., Jamali, M.A., and Yamamoto, H. (2006). Optimization Hole-Cutting Operations Sequence in CNC Machine Tools Using GA. *2006 International Conference on Service Systems and Service Management*, 501-506.

5. Ancau, M. (2009). The processing time optimization of printed circuit board. *Circuit World*, 35(3), 21-28.

6. Adam, A., Abidin, F.Z., and Ibrahim, Z. (2010). A Particle Swarm Optimization Approach to Robotic Drill Route Optimization. *2010 Fourth Asia International Conference on Mathematical/Analytical Modelling and Computer Simulation,* 60-64.

7. Zhu, G.Y. (2006). Drilling Path Optimization Based on Swarm Intelligent Algorithm. *2006 International Conference on Robotics and Biomimetics*, 193–196.

8. Narooei, K.D., Ramli, R., Abd-Rahman, M.N., Iberahim, F., and Qudeiri, J.A. (2014). Tool Routing Path Optimization fot Multi-Hole Drilling Based on Ant Colony Optimization. *World Applied Science Journal*, 32(9), 1894-1898.

9. Rodriguez, N.M., Ross, O.M., Sepulveda, R., and Castillo, O. (2012). Tool Path Optimization for Computer Numerical Control Machines based on Parallel ACO. *Engineering Letters*, 20(1).

10. Ross, O.M., Rodriguez, N.M., Sepulveda, R., and Melin, P. (2012). Methodology to Optimize Manufacturing Time for a CNC Using a High Performace Implementation of ACO. *International Journal of Advance Robotic System*, 9, 121_1-121_10.

11. Balakhrisnan, R., and Savaranan, M. (2017). Genetic Algorithm for TSP in Optimizing CNC Tool Path, International Journal of Engineering Technology. *Management and Applied Science*, 5(2), 13.9-14.6.

12. Shipacheva, E.N., Petunin, A.A., and Berezin, I.M. (2017). A genetic algorithm used for solving one optimization problem. *Proceeding of AIP Conference,* 1915, 040052_1-040052_4.

13. Al-Janan, D.H. and Liu, T.K. (2016). Path Optimization of CNC PCB drilling using hybrid Taguchi genetic algorithm. *Kybernetes*, 45(1), 107-125.

14. Lim, W.C.E., Kanagaraj, G., and Ponnambalam, S. (2014). PCB drill path optimization by combinatorial cuckoo search algorithm. *The Scientific World Journal*, 1-10.

15. Abdullah, H., Ramli, R., and Wahab, D.A. (2017). Tool path length optimisation for contour parallel milling based on modified ant colony optimisation. *International Journal of Advance Manufacturing Technology*, 92, pp. 1263-1276.

16. Qudeiri, J.E.A., Khadra, F.Y.A., and Al-Ahmari, A. (2013). GA Support System to Optimize the Sequence of Multi Level and Multi-Tool Operations in CNC Machines. *2013 14th ACIS International Conference on Software Engineering, Artificial Intelligence, Networking and Parallel/Distributed Computing*, 231-236.

17. Chen, J.C. and Zhong, T.X. (2002). A Hybrid-Coded Genetic Algorithm Based Optimisation of Non-Productive Paths in CNC Machining. *International Journal of Advance Manufacturing Technology*, 20, 163-168.

18. Mirjalili, S. (2016). SCA: A Sine Cosine Algorithm for solving optimization problems. *Knowledge-Based Systems*, 96, 120-133.

19. Santoso, B., and Willy, P. (2011). Metoda Metaheuristik: Konsep dan Implementasi. Surabaya, Indonesia: Prima Printing.

AASE
INTERNATIONAL CONFERENCE

AASE International Conference serves as platform that aims to provide opportunity to the academicians and scholars from across various disciplines to discuss interdisciplinary innovations. It's so happy to see the papers from all part of the world published in this proceedings. This proceeding brings out the various Research papers from diverse areas of science, engineering, technology, management, business and education. These articles that received for these conferences are very promising and impactful. We believe these studies have the potential to address key challenges in various sub domains of social sciences and applied sciences.